Eur. Phys. J. A **25**, s01, 397–402 (2005)
DOI: 10.1140/epjad/i2005-06-165-2

EPJ A direct
electronic only

Coulomb excitation of neutron-rich beams at REX-ISOLDE

H. Scheit[1,a], O. Niedermaier[1], V. Bildstein[1], H. Boie[1], J. Fitting[1], R. von Hahn[1], F. Köck[1], M. Lauer[1], U.K. Pal[1], H. Podlech[1], R. Repnow[1], D. Schwalm[1], C. Alvarez[2], F. Ames[2], G. Bollen[2], S. Emhofer[2], D. Habs[2], O. Kester[2], R. Lutter[2], K. Rudolph[2], M. Pasini[2], P.G. Thirolf[2], B.H. Wolf[2], J. Eberth[3], G. Gersch[3], H. Hess[3], P. Reiter[3], O. Thelen[3], N. Warr[3], D. Weisshaar[3], F. Aksouh[4], P. Van den Bergh[4], P. Van Duppen[4], M. Huyse[4], O. Ivanov[4], P. Mayet[4], J. Van de Walle[4], J. Äystö[5], P.A. Butler[5], J. Cederkäll[5], P. Delahaye[5], H.O.U. Fynbo[5], L.M. Fraile[5], O. Forstner[5], S. Franchoo[5,6], U. Köster[5], T. Nilsson[5,7], M. Oinonen[5], T. Sieber[5], F. Wenander[5], M. Pantea[7], A. Richter[7], G. Schrieder[7], H. Simon[7], T. Behrens[8], R. Gernhäuser[8], T. Kröll[8], R. Krücken[8], M. Münch[8], T. Davinson[9], J. Gerl[10], G. Huber[6], A. Hurst[11], J. Iwanicki[12], B. Jonson[13], P. Lieb[14], L. Liljeby[15], A. Schempp[16], A. Scherillo[3,17], P. Schmidt[6], and G. Walter[18]

[1] Max-Planck-Insitut für Kernphysik, Heidelberg, Germany
[2] Ludwig-Maximilians-Universität, München, Germany
[3] Institut für Kernphysik, Universität Köln, Köln, Germany
[4] Instituut voor Kern- en Stralingsfysica, University of Leuven, Leuven, Belgium
[5] CERN, Geneva, Switzerland
[6] Johannes Gutenberg-Universität, Mainz, Germany
[7] Institut für Kernphysik, Technische Universität Darmstadt, Darmstadt, Germany
[8] Technische Universität München, Garching, Germany
[9] University of Edinburgh, Edinburgh, UK
[10] Gesellschaft für Schwerionenforschung, Darmstadt, Germany
[11] Oliver Lodge Laboratory, University of Liverpool, UK
[12] Heavy Ion Laboratory, Warsaw University, Warsaw, Poland
[13] Chalmers Tekniska Högskola, Göteborg, Sweden
[14] Georg-August-Universität, Göttingen, Germany
[15] Manne Siegbahn Laboratory, Stockholm, Sweden
[16] Johann Wolfgang Goethe-Universität, Frankfurt, Germany
[17] Institut Laue-Langevin, Grenoble, France
[18] Institut de Recherches Subatomiques, Strasbourg, France

Received: 10 January 2005 /
Published online: 18 July 2005 –

Abstract. After the successful commissioning of the radioactive beam experiment at ISOLDE (REX-ISOLDE) —an accelerator for exotic nuclei produced by ISOLDE— in 2002 and the promotion to a CERN user facility in 2003, first physics experiments using these beams were performed. Initial experiments focused on the region of deformation in the vicinity of the neutron-rich Na and Mg isotopes. Preliminary results on the neutron-rich Na and Mg isotopes show the high potential and physics opportunities offered by the exotic isotope accelerator REX in conjunction with the modern Germanium γ spectrometer MINIBALL.

PACS. 25.70.De Coulomb excitation – 27.30.+t $20 \leq A \leq 38$ – 21.10.Re Collective levels

1 REX-ISOLDE

The Radioactive beam EXperiment (REX) [1,2,3] is a pilot experiment to demonstrate the feasibility of an efficient and cost-effective way to accumulate, bunch, charge breed, and accelerate radioactive exotic ions. In addition, beams of these nuclei should be produced for physics experiments, *e.g.* investigating the structure of nuclei far from stability. The REX accelerator is situated at the ISOLDE facility at CERN, which routinely provides a multitude of exotic nuclei for its users [4].

The main components of the REX accelerator are a trap (REX-TRAP), an ion source (REX-EBIS), a mass separator and the actual accelerator consisting of a radio frequency quadrupole, a re-buncher, an IH-structure, three 7-gap resonators and since 2004 a 9-gap IH-structure. REX-TRAP is a buffer-gas filled penning

[a] Conference presenter; e-mail: h.scheit@mpi-hd.mpg.de

trap that continuously traps the ions (with a charge state 1+) coming from the ISOLDE beam line. The accumulated ions are cooled and form bunches which are periodically (typically every 20 ms) transferred to the electron beam ion source REX-EBIS. Here charge breeding takes place and when a charge state to mass number ratio of $q/A > 1/4.5$ is reached the ions are extracted, mass separated (mainly to remove copious residual gas ions) and accelerated to energies around 0.8–3.1 MeV/u. It should be noted that in an EBIS the average charge state depends mainly on the breeding time and always a large fraction (about 15% for $A \sim 20$) of the ions is in one charge state. Still, as only one charge state of the ions can be accelerated, the largest reduction in transmission occurs after the EBIS. The total transmission from the ISOLDE target to the REX target is on the order of about 5%.

The first radioactive nuclear beam was accelerated in October 2001 to an energy of 2 MeV/u and in 2002 already several radioactive beams were produced with an energy of 2.2 MeV/u and used for commissioning experiments. First physics experiments using the accelerated exotic nuclei with a maximum beam energy of 2.2 MeV/u and 3.1 MeV/u were performed in 2003 and 2004, respectively. An upgrade to a beam energy of 4.3 MeV/u is planned in the near future, which will significantly extend the accessible region of nuclides toward heavier isotopes, especially for Coulomb excitation experiments. By the end of 2003 REX became a dedicated CERN user facility.

A picture of the setup in early 2002 is shown in fig. 1 with the MINIBALL array on the 65° beamline in the foreground.

Fig. 1. The REX-ISOLDE experimental hall in 2002. In the background the REX accelerator can be seen. After the bending magnet at the 65° the MINIBALL array is installed.

2 Experimental setup

The main experimental device currently used with REX is the MINIBALL HPGe array [5,6]. The array consists of 24 6-fold segmented, individually encapsulated, HPGe detectors arranged in 8 triple cryostats. The crystal geometry is shown in fig. 2. The detectors are mounted on an adjustable frame which allows for an easy adaptation of the geometry to the specific experimental requirements. The central core and six segment electrodes of each detector are equipped with a preamplifier with a cold stage and a warm main board. The charge integrated signals are subsequently digitized (12 bit, 40 MHz) and analyzed online and onboard the DGF-4C CAMAC card from XIA [7]. Besides energy and timing information the (user) algorithms implemented on the card [6,7,8,9,10] determine the interaction point of each γ-ray in the detector via pulse shape analysis (PSA), resulting in an about 100-fold increase in granularity in comparison to a non-segmented detector (the position resolution is about 7-8 mm FWHM, depending on the energy of the γ-ray). All digitizers run independently (receiving the same clock signal) and each single event is time stamped by a 40 MHz clock for offline event reconstruction.

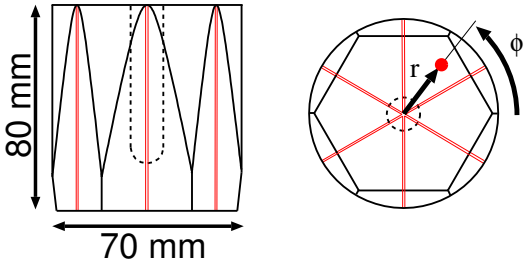

Fig. 2. MINIBALL HPGe crystal. The electrical segmentation is indicated.

In addition to the MINIBALL array an annular charged particle detector telescope (of CD type, see [11]) is employed consisting of a $\sim 500\,\mu$m thick ΔE followed by a $\sim 500\,\mu$m thick E detector. The ΔE detector is highly segmented (24×4 annular and 16×4 radial strips) to allow for a kinematic reconstruction of the events and covers an angular range from 15° to 50°. A parallel plate avalanche counter [12] was used to monitor the beam at zero degrees without stopping it, so that the (radioactive) beam particles are not deposited in the target area and reach the beam dump to reduce the radioactive decay background.

3 First experiments

The primary aim of REX and MINIBALL is the investigation of the development of the structure of nuclei far from

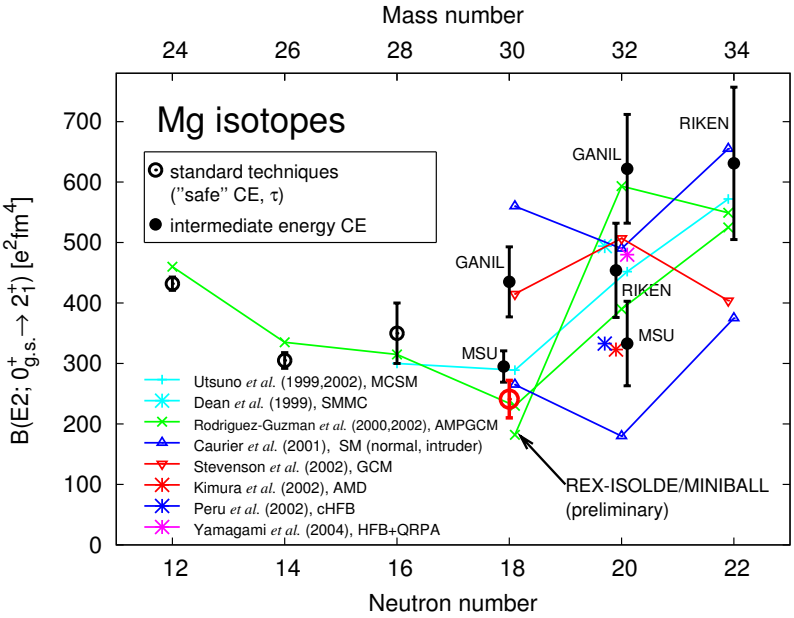

Fig. 3. $B(E2; 0^+_{gs} \rightarrow 2^+_1)$ values for the neutron-rich even-even magnesium isotopes. The values for ^{26,28}Mg were taken from [13].

stability. The reactions of choice to study the single particle and collective properties of nuclei with low-energy reaccelerated ISOL beams ($E_{beam} \sim$ Coulomb barrier) are single-nucleon transfer reactions and Coulomb excitation, respectively. Especially favorable for neutron-rich nuclei are (d, p) reactions (in inverse kinematics) on deuterated polyethylene targets, since here the cross sections are relatively high [14] and the neutron-pickup product is more neutron-rich by one neutron. By determining the differential cross sections to certain states as well as the angular distribution of the de-excitation γ-rays their spins and parities can be determined. From the absolute cross section, spectroscopic factors can be extracted.

An interesting region in the chart of nuclides is around the $N = 20$ nucleus ^{32}Mg. This region is well known as the island of deformation for almost 30 years [15,16], yet still, the knowledge on the nuclei in this region is very limited. Even today the extent of intruder ground state configurations in this region of the nuclear chart is not known. $B(E2; 0^+_{gs} \rightarrow 2^+_1)$ values for the even-even nuclei up to $N = 22$ (^{34}Mg) have been measured [17,18,19,20] rather recently, mainly by intermediate-energy Coulomb excitation at projectile fragmentation facilities. However, the data are very imprecise and measurements of different laboratories disagree by as much as a factor of two indicating that the systematic errors are not completely understood. The main contribution to the systematic error in these experiments is probably due to Coulomb-nuclear interference effects, which are always present at such high beam energies, even if the scattering angle of the projectiles is restricted to small values. Furthermore, the population of higher-lying states and subsequent feeding of the first 2^+ state also needs to be accounted for. In contrast, the Coulomb excitation studies at REX-ISOLDE are performed with beam energies well below the Coulomb barrier, yielding model independent results. In fig. 3 the theoretical and experimentally determined $B(E2; 0^+_{gs} \rightarrow 2^+_1)$ values for the neutron-rich Mg isotopes as a function of neutron number N are shown. It should be noted that all the theoretical results [21,22,23,24,25,26,27,28,29] are rather recent but give (nevertheless) very different values. Based on the data shown, a discrimination between the theoretical models is not possible.

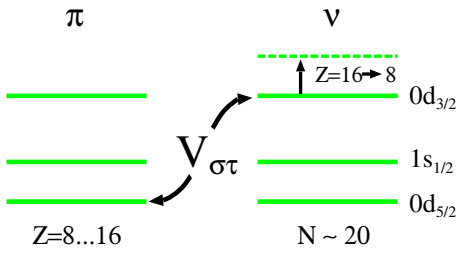

Fig. 4. Illustration of the $V_{\sigma\tau}$ interaction between neutron and proton orbitals with the same orbital angular momentum l and different total angular momentum j. This interaction was found to be very attractive for stable nuclei and rather weak for exotic neutron-rich nuclei, where the corresponding proton orbitals are often not filled, contributing to the appearance of new magic numbers [21].

Most information on the odd and odd-A nuclei stems from β decay experiments (see *e.g.* [30] and references therein) and in the future it will be attempted to measure ground state nuclear moments by the β NMR technique after polarization with a LASER beam [31,32].

In a recent publication Otsuka *et al.* [21] pointed out the importance of the $V_{\sigma\tau}$ (residual) interaction between orbits of the same orbital angular momentum, but with different total angular momentum between neutron and proton orbitals (see illustration in fig. 4 for the *sd*-shell). It is due to this interaction that the effective single particle

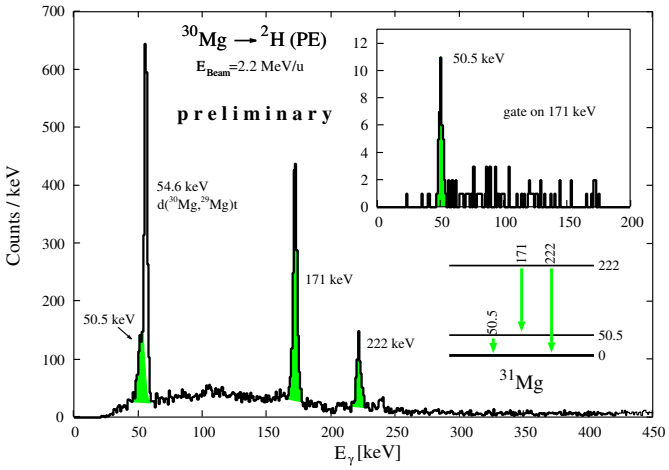

Fig. 5. γ spectrum coincident with any signal in the particle detector. Please note the almost negligible background and the extremely low-energy threshold of only 40–50 keV. The inset shows a γ energy spectrum in coincidence with the 171 keV line. As expected only the 50.5 keV transition is seen with still good statistics, demonstrating the high efficiency of the MINIBALL array.

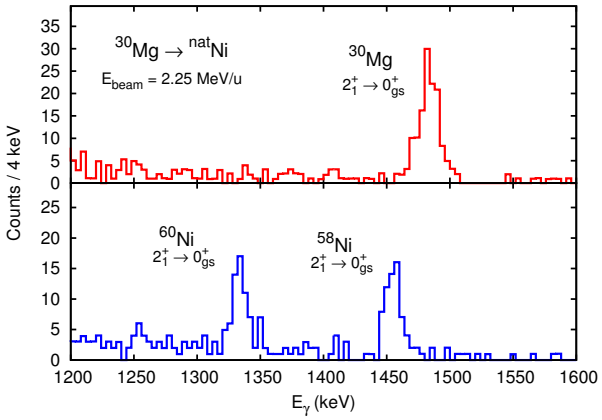

Fig. 6. Doppler corrected γ-ray spectra containing only events where ^{30}Mg projectiles were scattered in the CD detector. The upper panel shows the spectrum with Doppler correction for magnesium, while the lower panel the spectrum Doppler corrected for recoiling nickel.

energy (ESPE) of the $\nu d_{\frac{3}{2}}$ orbital is much lower in energy for stable nuclei, where the $\pi d_{\frac{5}{2}}$ orbital is nearly filled (resulting in a strong attraction of the orbitals) in comparison to very neutron-rich nuclei, where the $\pi d_{\frac{5}{2}}$ is nearly empty. ^{24}O ($\pi d_{\frac{5}{2}}$ completely empty), *e.g.*, shows features of a double magic nucleus due to the rise of the ESPE of the $\nu d_{\frac{3}{2}}$ orbital [21]. To further test the role of $V_{\sigma\tau}$ in the structure of these neutron-rich nuclei more precise experimental data are urgently needed.

At REX-ISOLDE with MINIBALL there is the possibility to study nuclei far from stability with standard nuclear physics tools (in inverse kinematics), which are not only well proven, but which also allow a direct comparison of the experimental results to ones obtained with stable beams. Therefore a program was started to systematically study the neutron-rich nuclei in this region via neutron-pickup reactions and Coulomb excitation.

4 Preliminary results

Preliminary γ energy spectra are shown in figs. 5 and 6 to demonstrate the quality of the spectra measured with a radioactive beam.

Figure 5 shows a spectrum taken in about 66 hours with a ^{30}Mg beam (4 neutrons away from stability with a halflife of only 335 ms) with an intensity of about $2 \cdot 10^4\,\mathrm{s}^{-1}$ ($E_{\mathrm{beam}} = 2.2\,\mathrm{MeV/u}$) on a 10 μm thick deuterated polyethylene foil. Several known transitions in ^{31}Mg can be seen, namely at 50.5 keV, 171 keV, and 222 keV. In addition a strong line at 54.6 keV is evident. This transition is coincident with tritons in the particle detector and corresponds therefore to the transition of the first excited state in ^{29}Mg (populated via the d(^{30}Mg, ^{29}Mg)t reaction) to the ground state. The inset shows a spectrum gated on the 171 keV line. As expected only the 50.5 keV transitions can be seen in this spectrum. The statistics is still rather good demonstrating the high efficiency of the MINIBALL array. Please note the very low background seen in these spectra, even though the beam particles are radioactive, and the extremely low-energy threshold of only 40–50 keV, which should be compared to a threshold of typically several 100 keV in experiments with fast beams.

For the Coulomb excitation study the ^{30}Mg beam provided by REX was incident on a natural nickel foil with a thickness of 1.0 mg/cm^2 located at the center of the scattering chamber. The measured γ-ray energy spectra obtained after 76 hours of data taking are shown in fig. 6, where peaks due to projectile and target excitation can be seen. The upper panel shows the γ spectrum obtained when the proper Doppler correction for ^{30}Mg is performed. The prominent peak at 1482 keV corresponds to the transition from the first 2^+ state to the ground state. When performing the Doppler correction for the recoiling nickel nuclei (bottom panel) the well known γ transitions at 1454 keV and 1333 keV, from the excitation and decay of the first excited 2^+ states in ^{58}Ni and ^{60}Ni, respectively, are evident. In the top/bottom spectrum the contribution of the peaks in the bottom/top spectrum is suppressed, *i.e.* the magnesium spectrum (top) does not include counts attributed to transitions in the nickel isotopes, since these counts correspond to wrongly Doppler corrected nickel γ-rays, and vice versa. Please note that the small change in peak area due to this procedure was taken into account in the extraction of the $B(E2)\uparrow$ value (see below). The two spectra contain only events where $A = 30$ nuclei were scattered into the CD detector. The recoiling nickel nuclei were separated from those by their lower kinetic energies at the same laboratory scattering angle.

For the extraction of the $B(E2)\uparrow$ value of ^{30}Mg only the events observed in coincidence with forward scattered ^{30}Mg were analyzed, ensuring safe surface distances D_{s} between projectile and target ranging from 6 fm to 23 fm [33].

Due to the occurrence of both projectile and target excitation the Coulomb excitation cross section σ_{CE} of the first excited 2^+ state in ^{30}Mg can be deduced relative to that of ^{58,60}Ni from the measured γ-ray yields N_γ alone

$$\sigma_{\mathrm{CE}}\left(^{30}\mathrm{Mg}\right) = \frac{\epsilon_\gamma(^{58,60}\mathrm{Ni})}{\epsilon_\gamma(^{30}\mathrm{Mg})} \cdot \frac{N_\gamma(^{30}\mathrm{Mg})}{N_\gamma(^{58,60}\mathrm{Ni})} \cdot \sigma_{\mathrm{CE}}\left(^{58,60}\mathrm{Ni}\right),$$

where ϵ_γ is the full energy peak efficiency (including the angular correlation of the emitted γ-rays) at the corresponding γ energy. The cross sections for the excitation of the nickel nuclei was calculated using the known spectroscopy [34,35,36] ($B(E2)\uparrow$ and quadrupole moments). For magnesium the $B(E2)\uparrow$ value was varied until the cross section was reproduced. The procedure was performed separately for the two nickel isotopes and the weighted average of the results was taken as the final value. For all measurements the γ yield of the two nickel isotopes was consistent with the natural abundance and the calculated Coulomb excitation cross section of the two isotopes. Even though the analysis presented above is straight forward a measurement with stable ^{22}Ne beam was performed for which the deduced $B(E2)\uparrow$ of 242(26) e^2fm^4 is in very good agreement with the adopted value [13] of 230(10) e^2fm^4 [1].

With the method proven the only difference to the measurement with a radioactive beam is a possible isobaric contamination. A contamination with a different mass is excluded due to the A/Q selection of the REX accelerator and the measurement of the total energy, which is proportional to the mass of the projectile, by the CD detector. There can be two sources of isobaric contamination, though: decay of ^{30}Mg during trapping and charge breeding and isobaric contamination directly released from and ionized at the primary ISOLDE target. The first contribution can be calculated from the known trapping and breeding time, which ranges from 12 ms to 32.4 ms, depending on the time, when a certain ^{30}Mg ion entered the trap. From the known lifetime of 483(25) ms an ^{30}Al contamination of 4.5% is calculated. The total ^{30}Al beam contamination and the contamination directly from the ISOLDE target[2] was investigated by the following methods:

- A LASER-on/off measurement was performed, where the RILIS LASER beam to the ISOLDE target was blocked periodically. During the LASER-off periods only surface ionized contaminants are extracted, while during the LASER-on periods, in addition, the (wanted) magnesium ions are extracted.
- The time dependence of the incident beam intensity with respect to the proton pulse impact on the ISOLDE target (T1) was analyzed. While a possible aluminum contamination is almost constantly present due to the long decay time of the release curve [39] the ^{30}Mg ions show a high intensity only for a short time after proton impact due to their fast release and short lifetime.
- The time dependence of the γ yield in the ^{30}Mg and ^{58,60}Ni peaks with respect to T1 was investigated to check what fraction of counts in the nickel peaks occurs during times, when there can be no ^{30}Mg in the beam.
- The Coulomb excitation of the first excited state in ^{30}Al at 244 keV was investigated.
- The γ yields due to β decay of ^{30}Mg and ^{30}Al were analyzed.

Table 1. Experimental $B(E2)\uparrow$ values in e^2fm^4.

	RIKEN		MSU	GANIL	REX-ISOLDE
Isotope	[17]	[20]	[18]	[19]	(preliminary)
^{30}Mg	–	–	295(26)	435(58)	241(31)
^{32}Mg	454(78)	449(53)	333(70) 440(55)	622(90)	–
^{34}Mg	–	631(126)	< 670	–	–

This analysis yields a value for the total beam contamination by ^{30}Al of 6.5% resulting in a correction of 5% of the nickel count rates. See [38] for details. In addition the time structure of the EBIS pulse was investigated and no peculiarities were found.

Including the determined beam impurities, a $B(E2;\ 0^+_{\mathrm{gs}} \rightarrow 2^+_1)$ value of ^{30}Mg of 241(31) e^2fm^4 was determined. The error is dominated by the statistical uncertainty, but also contains contributions due to the uncertainties of the $B(E2)\uparrow$ values of ^{58,60}Ni, the uncertainty in diagonal matrix elements for ^{30}Mg, a remaining uncertainty in the beam composition, the uncertainty due to angular distribution and possible reorientation of the emitted γ-rays [38].

Figure 3 shows the present value together with previously measured $B(E2)\uparrow$ values for the neutron-rich magnesium isotopes (see also table 1). While the initial goal was to confirm one or the other measurement for ^{30}Mg, it stands out that the $B(E2)\uparrow$ values of ^{30}Mg measured at MSU and GANIL are larger than the present value by about 20% and 80%, respectively (see also table 1).

While the source of this discrepancy is unknown it should be noted that in the intermediate-energy measurements with beam energies around 30–50 MeV/u several effects can influence the deduced $B(E2)\uparrow$ values such as feeding from higher-lying states and Coulomb-nuclear interference which have to be corrected. While the adiabatic cutoff limits the single-step excitation energy to values below 1–2 MeV in sub-barrier experiments, as presented here, in experiments with intermediate or relativistic beams, states up to several (5–10) MeV excitation energy can readily be populated [40]. Therefore, in these experiments any 2^+ (or even 1^-) state below 5–10 MeV can be excited and feeding of the first 2^+ state, unless it is corrected for, will result in an increased $B(E2)\uparrow$ rendering this type of measurement strongly model-*dependent*.

[1] The recently published $B(E2)\uparrow$ values for ^{58,60}Ni in [37] do not agree with this measurement and were not used (see [38]).

[2] Only aluminum can be present as it is easily surface ionized. Other isobars have a negligible yield (refractory of too short lived).

It is interesting to note that this feeding correction is performed differently by the different groups, ranging from no correction to corrections of more than 25%, sometimes based on experimental evidence of feeding [18], sometimes based on model calculations [17,19,20].

In conclusion, REX and MINIBALL are fully operational and first physics experiments focusing on the nuclear structure of the neutron-rich Na and Mg isotopes were performed. A preliminary analysis shows the high quality of the data that can be obtained with MINIBALL at REX-ISOLDE with a radioactive, low-energy and low-intensity beam. The analysis of the Coulomb excitation of a ^{30}Mg beam on a $^{\mathrm{nat}}$Ni target yields a $B(E2;\ 0^+_{\mathrm{gs}} \rightarrow 2^+_1)$ which is lower by about 20% and 80% that the MSU and GANIL results, respectively.

Support by the German BMBF (06 OK 958, 06 K 167, 06 BA 115), the Belgian FWO-Vlaanderen and IAP, the UK EPSRC, and the European Commission (TMR ERBFMRX CT97-0123, HPRI-CT-1999-00018, HRPI-CT-2001-50033) is acknowledged as well as the support by the ISOLDE Collaboration.

References

1. D. Habs *et al.*, Hyperfine Interact. **129**, 43 (2000).
2. O. Kester *et al.*, Nucl. Instrum. Methods B **204**, 20 (2003).
3. J. Cederkäll *et al.*, Nucl. Phys. A **746**, 17 (2004).
4. E. Kugler, Hyperfine Interact. **129**, 23 (2000).
5. J. Eberth *et al.*, Prog. Part. Nucl. Phys. **46**, 389 (2001).
6. D. Weisshaar, PhD Thesis, University of Cologne (2002).
7. `http://www.xia.com/`.
8. C. Gund, PhD Thesis, University Heidelberg (2000).
9. M. Lauer, Master's thesis, University Heidelberg (2001).
10. M. Lauer, PhD Thesis, University Heidelberg (2004).
11. A. Ostrowski *et al.*, Nucl. Instrum. Methods A **480**, 448 (2002).
12. J. Cub *et al.*, Nucl. Instrum. Methods A **453**, 522 (2000).
13. S. Raman, C.W. Nestor jr., P. Tikkanen, At. Data Nucl. Data Tables **78**, 1 (2001).
14. H. Lenske, G. Schrieder, Eur. Phys. J. A **2**, 41 (1998).
15. R. Klapisch *et al.*, Phys. Rev. Lett. **23**, 652 (1969).
16. C. Thibault *et al.*, Phys. Rev. C **12**, 644 (1975).
17. T. Motobayashi *et al.*, Phys. Lett. B **346**, 9 (1995).
18. B. Pritychenko *et al.*, Phys. Lett. B **461**, 322 (1999).
19. V. Chisté *et al.*, Phys. Lett. B **514**, 233 (2001).
20. H. Iwasaki *et al.*, Phys. Lett. B **522**, 227 (2001).
21. T. Otsuka *et al.*, Eur. Phys. J. A **15**, 151 (2002).
22. Y. Utsuno *et al.*, Phys. Rev. C **60**, 054315 (1999).
23. D.J. Dean *et al.*, Phys. Rev. C **59**, 2472 (1999).
24. R. Rodríguez-Guzmán, J. Egido, L. Robledo, Phys. Lett. B **474**, 15 (2000).
25. E. Caurier, F. Nowacki, A. Poves, Nucl. Phys. A **693**, 374 (2001).
26. S. Péru, M. Girod, J. Berger, Eur. Phys. J. A **9**, 35 (2000).
27. P. Stevenson, J. Rikovska Stone, M.R. Strayer, Phys. Lett. B **545**, 291 (2002).
28. M. Kimura, H. Horiuchi, Prog. Theor. Phys. **107**, 33 (2002).
29. M. Yamagami, N.V. Giai, Phys. Rev. C **69**, 034301 (2004).
30. S. Nummela *et al.*, Phys. Rev. C **64**, 054313 (2001).
31. M. Keim *et al.*, Eur. Phys. J. A **8**, 31 (2000).
32. M. Kowalska, these proceedings.
33. D. Schwalm, in *International School of Heavy Ion Physics: 3rd Course: Probing the Nuclear Paradigm with Heavy Ion Reactions*, edited by R. Broglia, P. Kienle, P.F. Bortignon (World Scientific, 1994) p. 1.
34. M. Bhat, Nucl. Data Sheets **80**, 789 (1997).
35. M. King, Nucl. Data Sheets **69**, 1 (1993).
36. P. Raghavan, At. Data Nucl. Data Tables **42**, 189 (1989).
37. O. Kenn *et al.*, Phys. Rev. C **63**, 064306 (2001).
38. O. Niedermaier *et al.*, Phys. Rev. Lett. **94**, 172501 (2005).
39. U. Köster *et al.*, Nucl. Instrum. Methods B **204**, 347 (2003).
40. K. Alder, A. Winther, *Electromagnetic Excitation: Theory of Coulomb Excitation with Heavy Ions* (North-Holland, 1975).